Supplement of Atmos. Chem. Phys., 20, 7459–7472, 2020
https://doi.org/10.5194/acp-20-7459-2020-supplement

Atmospheric Chemistry and Physics
Open Access
EGU

Supplement of

Long-term brown carbon and smoke tracer observations in Bogotá, Colombia: association with medium-range transport of biomass burning plumes

Juan Manuel Rincón-Riveros et al.

Correspondence to: Ricardo Morales Betancourt (r.moralesb@uniandes.edu.co)

A BrC-BC Attribution model

There are several different methods to decompose the light-absorption coefficient of carbonaceous material between what is typically referred to as Black Carbon and the fraction that comes from biomass burning, which we will refer to as Brown Carbon. In this work, we applied the method described by Sandradewi et al., (2008). The equations involved in this method are briefly described here. The fundamentals of the Sandradewi et al., (2008) method is that absorption at any given wavelength (measured by the Aethalometer) is decomposed as the sum of two components:

$$b_{abs}(\lambda_1) = b_{FF}(\lambda_1) + b_{BB}(\lambda_1) \tag{S.1}$$

$$b_{abs}(\lambda_2) = b_{FF}(\lambda_2) + b_{BB}(\lambda_1) \tag{S.2}$$

where $b_{FF}(\lambda_i)$ is the absorption attributed to Fossil Fuel burning, while $b_{BB}(\lambda_i)$ is the absorption due to biomass burning. Additionally, it is assumed that the absorption from FF at different wavelengths is related to a specific Angstrom exponent, called α_{FF}. A similar assumption is made for absorption from BB, with a specific Angstrom absorption exponent α_{BB}. This is expressed as

$$\frac{b_{ff}(\lambda_1)}{b_{ff}(\lambda_2)} = \left(\frac{\lambda_1}{\lambda_2}\right)^{-\alpha_{ff}} \tag{S.3}$$

$$\frac{b_{wb}(\lambda_1)}{b_{wb}(\lambda_2)} = \left(\frac{\lambda_1}{\lambda_2}\right)^{-\alpha_{wb}} \tag{S.4}$$

Equations S.1 to S.4 form a system of four equations and six unknowns. However, if the values of α_{FF} and α_{BB} are known (or assumed), then, its possible to solve the system the remaining four unknowns. Solving for $b_{BB}(\lambda_2)$ and naming $r = \lambda_1/\lambda_2$,

$$b_{BB}(\lambda_2) = r^{\alpha_{BB}} \frac{(b_{abs}(\lambda_1) r^{\alpha_{FF}} - b_{abs}(\lambda_2))}{r^{\alpha_{FF}} - r^{\alpha_{BB}}} \tag{S.5}$$

Similarly, the other three unknowns can be solved for in terms of the measured absorptions $b_{abs}(\lambda_i)$ and the parameters α_{BB} and α_{FF}. This expression can be further simplified if one is interested in the fraction of absorption attributed to a given source. Defining the fraction attributable to Biomas Burning as f_{BB}, and using the definition of the absorption Angstrom exponent α, we have

$$f_{BB} = \frac{b_{abs,BB}(\lambda_1)}{b_{abs}(\lambda_1)} = \frac{\left(\frac{\lambda_1}{\lambda_2}\right)^{\alpha-\alpha_{FF}} - 1}{\left(\frac{\lambda_1}{\lambda_2}\right)^{\alpha_{FF}-\alpha_{BB}} - 1} \tag{S.6}$$

In this way, the fraction f_{BB} can be calculated exclusively as a function of the Angstrom exponent α, and the parameters α_{BB} and α_{FF}. A similar procedure can be applied to solve for the other unknowns. Once f_{BB} is determined, then, from Equation S.6 is clear that the absorption attributable to BB can be simply expressed as:

$$b_{abs,BB}(\lambda_1) = b_{abs}(\lambda_1) \times f_{BB} \tag{S.7}$$

B Sensitivity analysis

To determine the sensitivity of our method of analysis, we performed a sensitivity test by varying the set parameters α_{FF} and $_{BB}$. To this end, we allowed variations of $\alpha_{FF} = 1.0 \pm 0.1$, as this parameter is known to be close to one. For α_{BB} a wider range of variation was allowed, $\alpha_{BB} = 2.0 \pm 0.4$. As is clear from Equation S.7, the absolute value of $b_{abs,BB}(\lambda_1)$ and correspondingly, that of the inferred BrC concentration (i.e., BrC$\sim b_{abs,BB}$), will change. to determine how large of a change could be expected, we calculated BrC for a combination of the perturbed α_{FF} and α_{BB} parameters for the high and low BB acitivity seasons. Results are shown in Figure S.1. Although there are clearly some variations in BrC for each set of parameters used, in all cases considered, there is also a statistically significant difference between the DJF and JJA values, wih much larger concentrations during DJF than JJA. This shows that although sensitivity to parameters does impact inferred BrC concentration, the observed seasonal changes are observable irrespective of parameter choice.

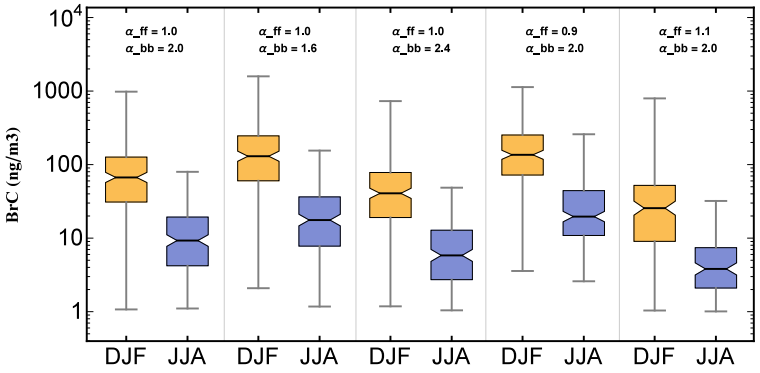

Figure S.1: Seasonal distribution of BrC for DJF and JJA, using different α_{FF} and α_{BB} parameter combintations.

Similarly, we analyzed the impact that the choice of wavelength pair to compute α has on the time series structure of the inferred $b_{abs,BB}$ values. This is shown in Figure S.2. The cross-correlation between time series is larger than 0.97 in all cases. Therefore, although there is indeed a change in the absolute value of $b_{abs,BB}$, the temporal variations remain unchanged. This, in turn, means that the results of the correlation analysis between $b_{abs,BB}$ and fire counts, or levoglucosan or WSOC measurements, are independent of the specific wavelength

chosen. They are also independent of the pair of wavelengths selected to apply the decomposition.

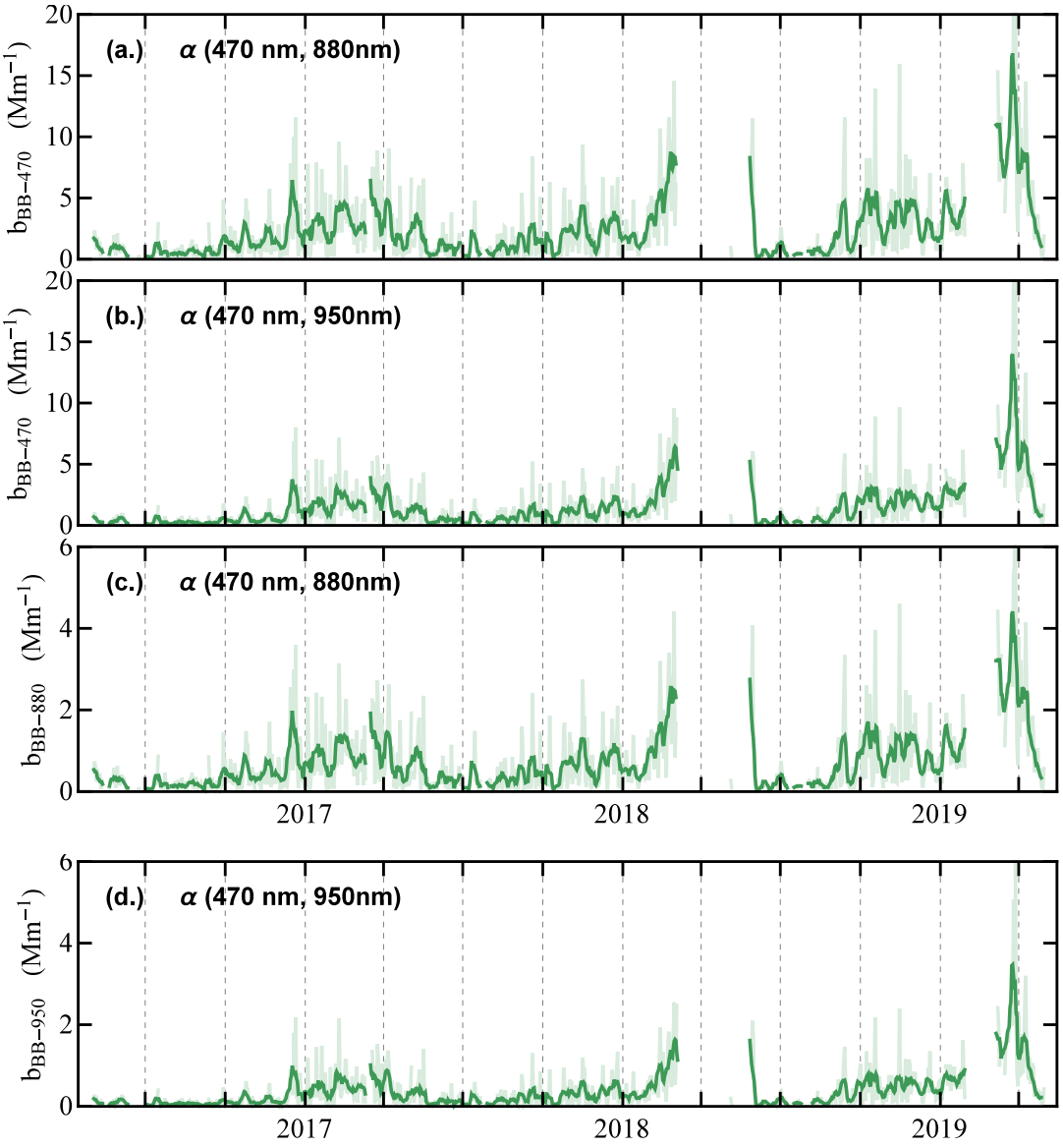

Figure S.2: Figure S2. Time series of $b_{abs,BB}$ at different wavelengths and computed with different pairs of wavelenghts. (a.) $b_{abs,BB}(450nm)$ for $\alpha_{450,880}$, (b.) $b_{abs,BB}(450nm)$ for $\alpha_{450,950}$, (c.) $b_{abs,BB}(880nm)$ for $\alpha_{450,880}$, and (d.) $b_{abs,BB}(950nm)$ for $\alpha_{450,950}$

C Diurnal Cycle of Black Carbon and Mixing Layer Height

Urban ambient Black Carbon (BC) concentrations were determined from hourly data from 6 stations in Bogotás Air Quality Monitoring Network. The BC is collected with Aethalometers model AE33. During the same period, Black Carbon data was collected at the Monserrate Sanctuary site as described in detail in the Methods section of the main manuscript. The daily mean profile for both datasets is shown in Figure S1. This analysis shows an overall similar diurnal profiles, with peak concentrations observed in the morning, likely associated to rush-hour traffic emissions. The mean ratio between ambient and background concentrations is 0.15. The similarity between both profiles, however, and the presence of a morning peak at the Monserrate site, suggests observations at the site are strongly impacted by urban emissions.

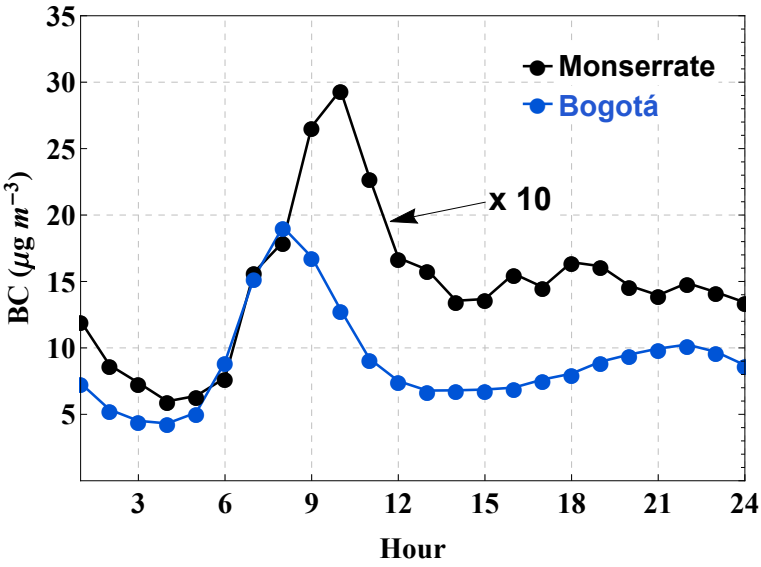

Figure S.3: Hourly mean Black Carbon concentration measured at the Air Quality Monitoring Station Network of Bogot (Blue) and at the Monserrate Sanctuary site (Black).

The two-hour lag between these two signals is likely produced by the altitude difference between the two measurement sites and the mixed layer morning expansion. To confirm this hypothesis, we analyzed mixing layer height (H_{mix}) from Bogotás airport atmospheric sounding data. There is typically one ra-

diosonde launch per day. Hourly H_{mix} was estimated by adding the difference between the hourly surface temperature recorded at the ground to the surface temperature reported in the radiosonde data. There is typically one radiosonde launch daily at 12Z (7:00 am local time). The Mixing Height is then computed as the height at which the temperature of a dry-adiabatically lifted air parcel with temperature equal to the hourly reported surface temperature intersects the 12Z temperature prole. This is a modication of the method of Holzworth (1967), which was conceived with a focus on air quality applications. This was performed for all available data during the three-year monitoring period, and then, hourly mean values were computed. Figure S.4 shows the hourly mean estimate of H_{mix} according to the method described. The mixing height exceeds the Monserrate site altitude between 8.30 am and 9:00 am, roughly two hours after the beginning of the convective layer expansion.

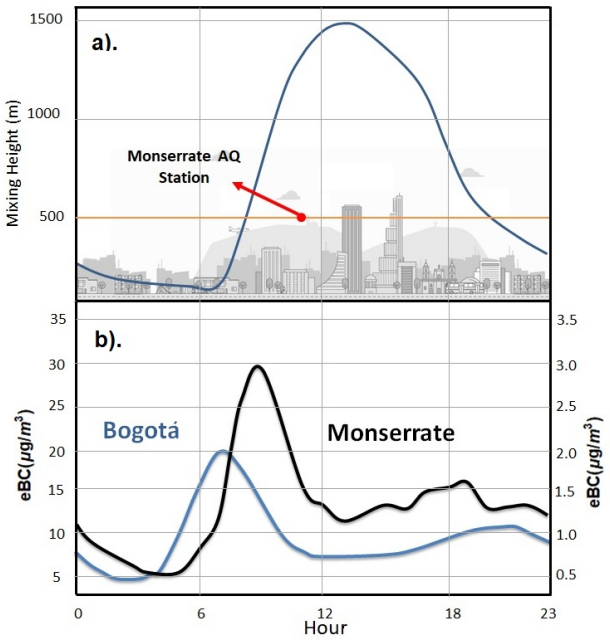

Figure S.4: Mean hourly mixing height according to the 12Z radiosonde temperature profile and hourly surface temperature reported in Bogotá. The Monserrate site height is depicted as the orange dashed line.

D Annual Cycle of Daily Fire Countst

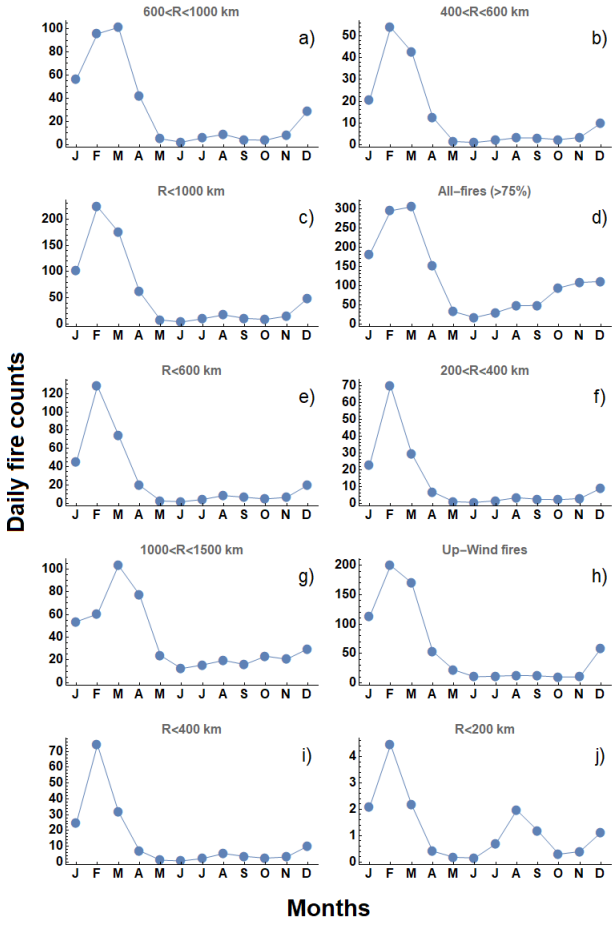

Figure S.5: Annual profile for all fire counting considered in the article.

As described in detail in the manuscript (Section 2.4), we applied several methods to count the number of fires and produce time series of daily fire counts. We considered buffer-radii of 200 km, 400 km, 600 km, 1000 km, and 1500 km from Bogotá, and selected only those fires within that region. Additionally, annular regions, those formed between circular buffers of different radius were analyzed to identify specific emission areas in relation to their distance to Bogot. Figure S3 shows mean monthly variation for number of daily fire counts for each buffer area identified for entire monitoring period. This analysis concludes counting types that includes farthest active fires (e.g. Figure S.5a,

S.5d, S.5g) have the maximum peak in March, same month whit BrC highest concentrations.

E Brown Carbon, Black Carbon, and Smoke tracer observations

We carried out three field campaigns, two during the high biomass burning activity season (Campaigns C1 and C3) and one during a low fire activity season (Campaign C2). During those campaigns, PM2.5 filter samples were collected and analyzed for smoke tracers levoglucosan, water-soluble organic carbon (WSOC), and water-soluble potassium (WSK). Additional analysis to determine elemental and organic carbon were carried out. Elemental carbon concentrations were compared against on-line Black Carbon observations. The tracers were detected in concentrations above the limit of detection in every campaign, and good agreement was observed between chemical and optical measurements for both smoke tracers and fossil fuel tracers.

Figure S.6 shows the time series of continuous Brown Carbon and Black Carbon observations at the Monserrate Site, as well as the daily mean concentration of the filter-based smoke tracers that were analyzed.

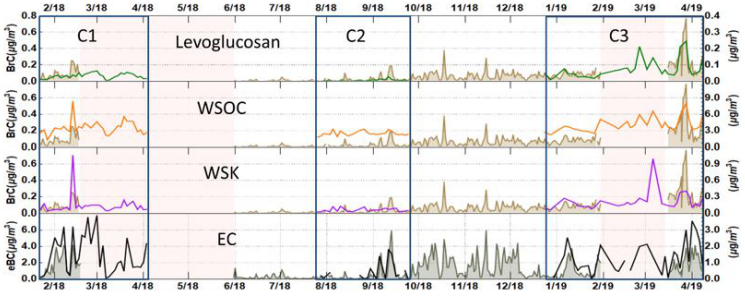

Figure S.6: Daily time series of Brown Carbon (Brown, in the first three panels), Black Carbon (Gray, in the lowermost panel) for the entire observation period. Levoglucosan (green, upper panel), WSOC (Orange, second panel), WSK (Purple, third panel), and EC (Black, lower panel), are included for the three filter sampling campaigns carried out. Letters C1, C2, and C3 mark the periods of filter samples collection.

F Biomass burning emissions footprint

In order to identify the spatial distribution biomass burning aerosol sources that could affect Bogotás air quality, we paired the in-situ BrC concentrations observed at the Monserrate Site, HYSPLIT back-trajectories, and MODIS detected fires to apply two different methodologies. Concentration Weighted Trajectory (CWT) is a widely used method to determine spatial distribution of sources in air quality applications. In this procedure (Equation S.8), each grid cell in the domain is assigned a concentration obtained by weighting measured receptor-site concentrations by the residence time of associated back-trajectories that crossed that grid cell (Siebert, 1994), i.e.,

$$\bar{C}_{ij} = \frac{\sum_{k=1}^{N} C_k \tau_{ijk}}{\sum_{k=1}^{N} \tau_{ijk}} \tag{S.8}$$

In Equation S.8, $\bar{C}_{ij}$ is the average concentration assigned to grid cell (i, j), C_k is the concentration recorded at Monserrate site in day k, τ_{ijk} is the residence time in the cell (i, j) of a back-trajectory arriving at the receptor site in day k, and the summation is over all sampling days N.

In our analysis, we separated the observation period in seasons, namely DJFM (high-BB season), AMJJ (low-BB season), and ASON (transition period). The result of applying Equation 1 to these seasons for the three years of BrC data is shown in Figure S.7a, S.7c, and S.7e. The spatial distribution is strongly influenced by the seasonal wind patterns. During DJFM, longer trajectories are observed because the southward displacement of the ITCZ causes the region to be in the trade-wind regime. Therefore, DJFM has both, high-BB activity and winds blowing from those source regions towards the receptor. The second period, AMJJ, has the lowest fire activity and a clear wind direction predominance from south and west, i.e., away from the potential source regions. The third period (ASON) has no dominant wind direction, with short trajectories and therefore high density of trajectories in the vicinity of Bogotá. The highest BrC concentrations are assigned close to the city, this, likely due to the high density of trajectories crossing those grid cells. This methodology attributes concentrations depending trajectories density and beyond continental areas, this attributions does not identify sources that could emit BrC to the atmosphere.

After identifying the above mentioned limitations when the CWT methodology is applied, we developed a variation of this method that allows us to relate

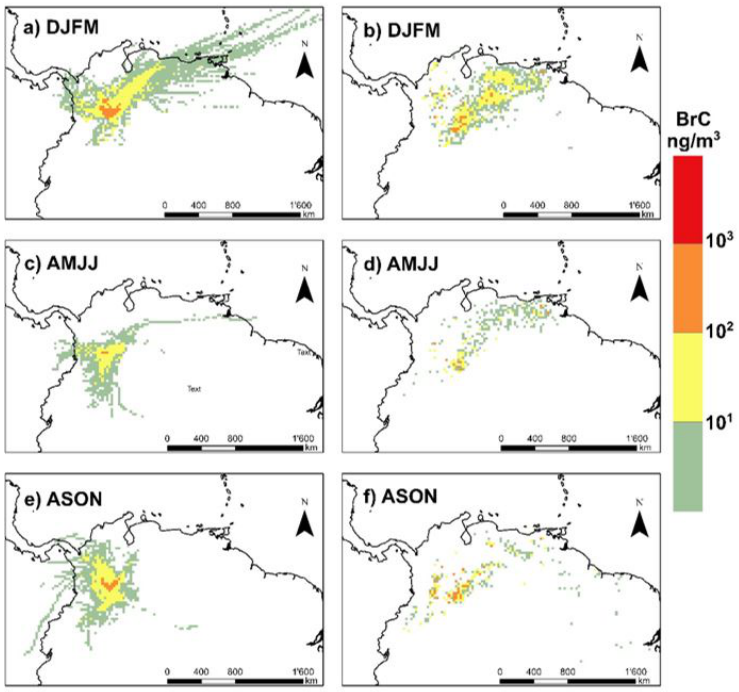

Figure S.7: Mean Brown Carbon concentrations, $\bar{C}_{i,j}$, after applying the spatial allocation algorithms described by Equation 1 (panels a., c., and d.) and Equation 2 (panels b., d., f.).

the measured concentrations to the origin of the emissions. We performed two modifications to Equation 1. First, we calculated the Fire Radiative Power (FRP) for MODIS hot-spots that were within a 150 km buffer of the back-trajectory location. This is, we defined the variable FRP_{ijk} as the sum of the FRP for all individual fires in grid cell (i, j) that were within a 150 km radius of the location of a back-trajectory arriving at the receptor site on day k. Additionally, we applied a dilution term, in which an exponential decay in term as air masses travel towards the receptor. Therefore, in this method, $\bar{C}_{ij}$ is calculated as

$$\bar{C}_{ij} = \frac{\sum_{k=1}^{N} C_k \mathrm{FRP}_{ijk} e^{-t/\tau}}{\sum_{k=1}^{N} \mathrm{FRP}_{ijk} e^{-t/\tau}} \tag{S.9}$$

The term $e^{(}-t/\tau)$ in Equation S.9 accounts for dilution. The dilution timescale was assumed to be 5 days, i.e., $\tau = 5$ days. Unlike the CWT methodology,

the new Concentration Trajectory Weighted by FRP methodology identifies specific areas where the MODIS sensor usually identifies large-scale active fires over which air masses eventually reaching the measurement site pass by. Therefore, those areas could be potential sources with impact on the BrC concentrations measured in Bogot. The results of applying this method for the three years of measurements are shown in Figure S.7b, S.7d, and S.7f. The resulting spatial footprint of Biomass Burning sources clearly suggest that open biomass burning in the eastern savannas of the Orinoco river basin are the most up-wind significant sources of smoke for our measurement site.